Electronic Supplementary Material (ESI) for Chemical Science.

Supporting Information

Conductivity and Photoconductivity in a Two-Dimensional Zinc Bis(triarylamine) Coordination Polymer

Chin May Ngue*, Kuan Fu Ho, Batjargal Sainbileg, Erdembayalag Batsaikhan, Michitoshi Hayashi, Kuei Yi Lee, Ruei San Chen*, Man Kit Leung*

Dr. Chin May Ngue and Prof. Man Kit Leung
Department of Chemistry, National Taiwan University, Taipei 106, Taiwan

Kuan Fu Ho and Prof. Kuei Yi Lee
Graduate Institute of Electro-Optical Engineering, National Taiwan University of Science and Technology,
Taipei 106, Taiwan

Prof. Ruei San Chen
Graduate Institute of Applied Science and Technology, National Taiwan University of Science and Technology,
Taipei 106, Taiwan

Dr. Batjargal Sainbileg, Dr. Erdembayalag Batsaikhan and Prof. Michitoshi Hayashi
Center for Condensed Matter Sciences, National Taiwan University, Taipei 106, Taiwan;
Center of Atomic Initiative for New Materials, National Taiwan University, Taipei 106, Taiwan

Table of Contents

Figure S8. SEM image of **1**, platinum microelectrode fabricated using focus ion beam (FIB) at both crystal edges.

Figure S9. a) and c) Photocurrent response when time as a function at wavelength excitation of 532 nm and 633 nm, b) and d) photocarrier lifetime fitting at 532 nm and 633 nm.

Table S2. Length, width, and thickness of **1** under different batches.

Figure S10. Nitrogen sorption isotherm of **1**. Brunauer-Emmett-Teller surface area is 12.83 m^2/g.

Table S3. Compilation of photoconductive gain for semiconductors.

Figure S11. a) and c) Photocurrent response when time as a function at wavelength excitation of 532 nm and 633 nm, b) and d) photocarrier lifetime fitting at 532 nm and 633 nm.

6) Formula for Responsivity and Photoconductive Gain

1) Materials

Zinc(II) chloride (Sigma-Aldrich, reagent grade, 98%), diphenylamine (Acros, 99%), 1,4-dibromobenzene (Acros, 99%), sodium tert-butoxide (Thermo Scientific, 99%), Palladium (II) acetate (UR-IPAL002, 99%), pyridine-4-boronic acid (Matrix Scientific, 95%), $Pd(PPh_3)4$ (Acros, 99%), $P(t\text{-}Bu)_3(HBF_4)$ (AK scientific, 97%), DMF (JT baker, HPLC grade), acetonitrile (J.T. Baker, HPLC grade), chloroform (Merck), toluene (ECHO, ACS grade) and 1,4-dioxane (Acros, 99.5%)

Electrochemistry: Calcium hydride (Acros, ca. 93% 10-100 mm), ferrocene (Acros, 98%), tetra-*n*-butylammonium hexafluorophosphate (Alfa Aesar, 98%)- recrystallization using ethanol before use.

NMR: $CDCl_3$ (Sigma-Aldrich), C_6D_6 (Sigma-Aldrich)

2) Instrumentation

Elemental analyses (C, H, N) *via* combustion were performed using an Elementar Vario cube analyzer at the MOST Instrumental Center at National Taiwan University (NTU), Taipei, Taiwan. Thermogravimetric analysis was performed using a TA Instrument Q50 Thermogravimetric Analyzer. Measurements were carried out at the temperature of 30 °C to 900 °C with a ramp of 10 °C per min under a nitrogen atmosphere. Powder X-ray diffraction data were collected on a Bruker D8 Advance powder diffractometer at 40 kV and 40 mA operating at the Cu K_α wavelength (1.5406 Å). The Zn sample was placed on a zero-background silicon crystal plate. Diffuse reflectance spectra were collected on an ultraviolet−visible (UV−vis) spectrometer JASCO V670 in the range of 300−1200 nm. Barium sulfate ($BaSO_4$) was used to obtain a baseline spectrum. Y axis spectra were recorded as the Kubelka-Munk transform, where $F(R) = (1\text{-}R)^2/2R$. IR spectra were recorded in the range of 4000-400 cm^{-1} on a PerkinElmer Paragon 100 FT-IR spectrometer using the KBr disc technique. ^1H NMR spectra were obtained on a Bruker Advance 400 MHz spectrometer at 298 K.

Conductivity Measurement

Two-contact probe single crystal measurements

Crystals were dried to eliminate the trapped solvents. Good quality single crystals of Zn compound with a length of a few μm with no visible defects were carefully selected under an optical microscope. The selected crystals were spread over an insulating SiO_2 (300 nm)/*n*-Si templates with the assistance of an optical microscope that was pre-patterned with a Ti/Au electrode. The Ti/Au electrode is an interconnection between the micrometer-sized single crystals. Both ends of the single crystal were fabricated with a platinum electrode. The fabrication of Pt microelectrode using a focused-ion beam (FIB) technique. The applied voltage and current were 30 kV and 100 pA, respectively. The lengths and widths of the crystals were estimated using field-emission scanning electron microscopy (FESEM). The thickness of the single crystals was measured using atomic force microscopy (AFM). IV curve was measured using Keithley 4200-SCS. The temperature-dependent conductivity measurement was performed at an ultralow current leakage cryogenic probe station (Lake Shore Cryotronics TTP4).

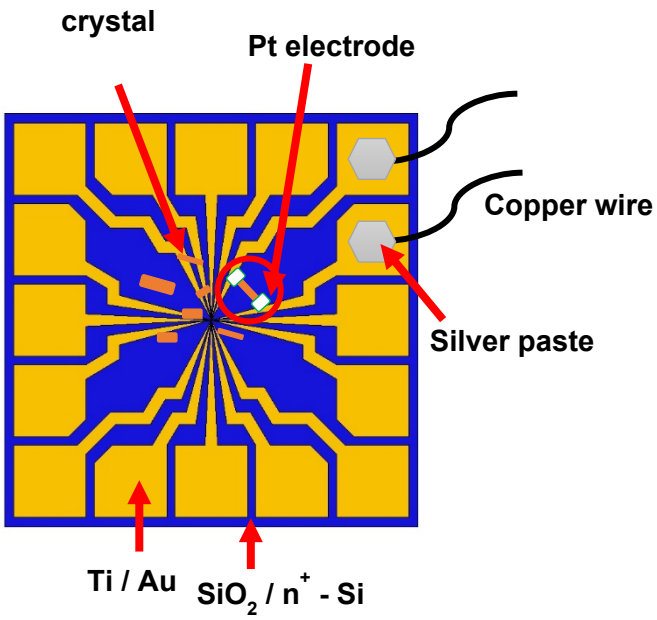

Determination of conductivity and activation energy

A two-contact probe single-crystal method was adopted to measure the conductivity. The I-V curves were obtained with an applied voltage from -1 V to 1 V. Conductivity value (S/cm) was calculated using Equation S1. [1] *I* (A) is the current, *V* (V) is the voltage across the pellet, *L* (cm) is the length, and *A* (cm^2) is the cross-sectional area. I/V value was extracted from the slope of the I-V curve.

$$\sigma = \frac{I}{V}\ \frac{L}{A} \qquad \text{Eq. S1}$$

To measure the activation energy, the I-V curve was measured from 30 K to 300 K to obtain the conductivities under the function of temperatures. The conductivity temperature was fitted using the Arrhenius model. The equation S2 is the Arrhenius formula,

$$\sigma = \sigma_0 e^{-\frac{Ea}{KBT}} \qquad \text{Eq. S2}$$

where σ is the conductivity, σ_0 is the pre-exponential factor, E_a is the Arrhenius activation energy, k_B is the Boltzmann constant, and T is the temperature. Equation S2 can be rearranged as:

$$\ln(\sigma) = \ln(\sigma_0) - \frac{1}{T}\frac{Ea}{kB} \qquad \text{Eq. S3}$$

Plotting the natural log, ln (σ), to the reciprocal temperature of 1000/T, K^{-1} we obtained the slope value of $-\frac{Ea}{kB}$.

Photoconductivity Measurements

A Nd:YAG laser (λ = 532 nm) and the diode lasers (λ = 405nm and 633nm) were used as the excitation sources for the photoconductivity measurements. A UV holographic diffuser was used to broaden the laser beam size (~25 mm^2) to minimize errors in light intensity calculations. The incident laser power was measured by a calibrated power meter (Ophir Nova II) with a silicon photodiode head (Ophir PD300-UV).

Lifetime Measurements

A multi-functional time-resolved photoconductivity (TRPC) measurement system (Unique TR01A) with the optimal response time resolution reaching 4 ns with a light source of 405 nm, 532 nm and 633 nm wavelength was utilized to characterized the photoresponse signals and carrier lifetime of **1**.

Cyclic Voltammetry

Cyclic voltammograms were obtained by using a CH Instrument 611B electrochemical analyzer. The acetonitrile and dichloromethane were distilled over CaH_2 and P_2O_5, respectively, prior to the electrochemical experiments. Measurements were carried out in a three-electrode system. Glassy carbon was used as the working electrode, platinum wire as an auxiliary electrode, and Ag/AgCl as a reference electrode. The Zn compound was mounted onto the glassy carbon electrode. The ligand was directly dissolved in the organic solvent. The electrolyte used in this work is 0.1 M ([*n*-Bu_4N]PF_6). Oxygen was removed by bubbling with Argon gas for 20 min. The voltammograms were acquired from the unstirred solution under an atmosphere of Argon gas. Ferrocene served as an internal reference and was added at the last measurement.

Computational details

First-principles DFT calculations were performed by implementing the Vienna Ab initio Simulation Package (VASP, version 5.4.4) within the framework of plane-wave and PAW pseudopotential methods.[2] The exchange-correlation function was treated with spin-polarized PBE+U (U = 2 eV), including Grimme's D3 dispersion interactions for SCF and geometry optimization calculations whereas the Heyd−Scuseria−Ernzerhof (HSE06) hybrid functional was used for calculations of electronic properties.[3] The Monkhorst-Pack 8 × 8 × 8 k-meshes for a sampling of irreducible Brillouin Zone and the 520 eV cut-off for plane-wave basis were used in the calculations. The experimentally defined crystal structure of **1** was relaxed until the total energy of the system was less than 1 μeV, and the forces on atoms were less than 1 meV/Å.

3) Synthesis of materials

Synthesis of *N¹, N¹, N⁴, N⁴-tetraphenylbenzene-1,4-diamine* [4]

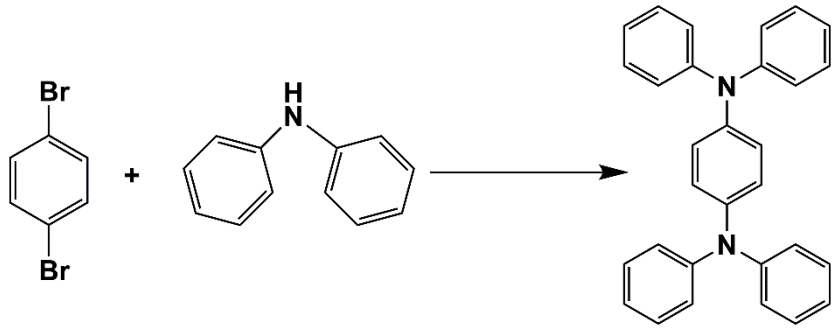

A dry 100 mL two-neck round-bottomed flask was prepared. 1,4-dibromobenzene (2.36 g), diphenylamine (4.24 g), NaO^tBu (2.40 g), $Pd(OAC)_2$ (112.3 mg), $P(t\text{-}Bu)_3(HBF_4)$ (436 mg) and dry toluene 80 mL. Before adding toluene, the mixture was evacuated and purged with Argon gas three times. The toluene was transferred under the Argon atmosphere. The reaction mixture was refluxed overnight under a stream of Argon. After cooling down to room temperature, white crystalline solids were precipitated out. The white solids were filtered out (5.18 g, 88.5 %). ^1H NMR (400 MHz, C_6D_6, ppm): δ 7.11 (dd, 8H), δ 7.04 (t, 8H), δ 6.96 (s, 4H), δ 6.82 (t, 4H).

Synthesis of *N¹, N¹, N⁴, N⁴-Tetrakis(4-bromophenyl)benzene-1,4-diamine* [5]

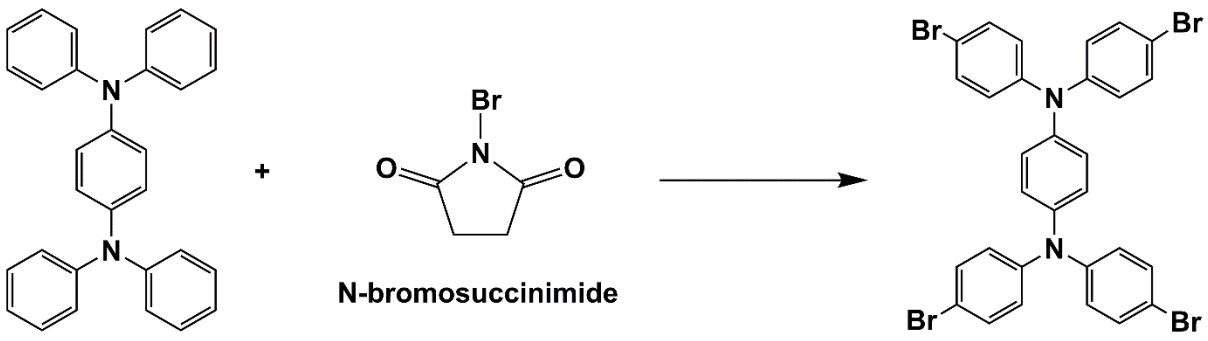

N^1, N^1, N^4, N^4-tetraphenylbenzene-1,4-diamine (1.00 g, 1 equiv.) and 40 mL of DMF were transferred to a two-neck round bottom flask of 100 mL. The reaction mixture was cooled in an ice bath at 0 °C. *N*-bromosuccinimide (1.94 g, 4.5 equiv.) was dissolved in 20 mL DMF and added dropwise for about 30 mins using a dropping funnel. After 30 mins of addition, the reaction mixture was kept and continued stirring at 0 °C for 30 mins. After that, it was warmed up to room temperature. A green suspension was observed. After stirring overnight, the purple suspension was obtained. DI water (500 mL) was poured onto the suspension. A grey precipitate was collected *via* filtration and recrystallized using chloroform (150 mL). A white powder was isolated after recrystallization by chloroform (0.93 g, 52.5 %). ^{1}H NMR (400 MHz, $CdCl_3$): δ 7.34 (d, 8H), δ 6.94 (m, 12H).

Synthesis of *N^1,N^1,N^4,N^4*-tetrakis(4-(pyridin-4-yl)phenyl)benzene-1,4-diamine (TPPB)

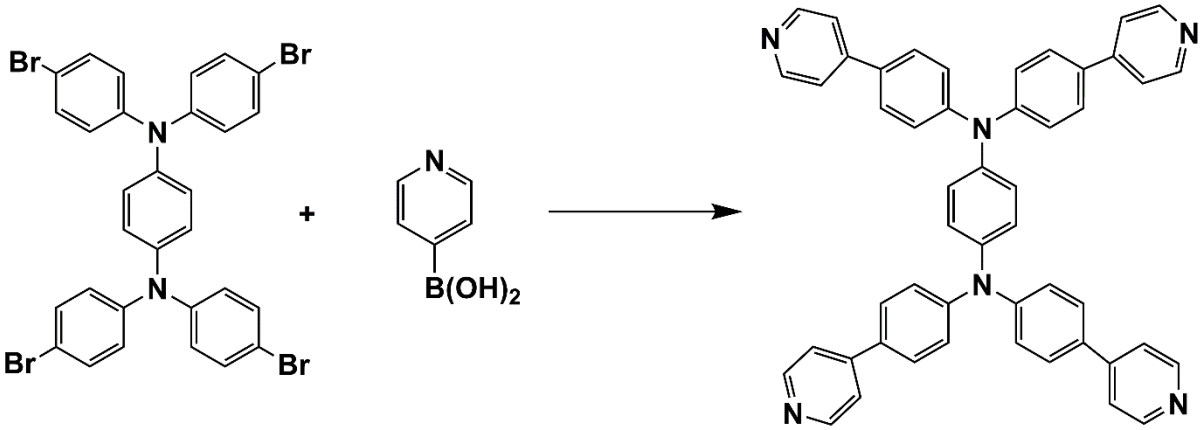

A 150 mL two-neck round bottom flask was charged with N^1, N^1, N^4, N^4-Tetrakis(4-bromophenyl)benzene-1,4-diamine (1 g), pyridine-4-boronic acid (1.2 g), K_2CO_3 (1.3 g), $Pd(PPh_3)_4$ (120 mg). The air was evacuated and purged with Argon gas three times. 1,4-dioxane/water (3:2) were added. The reaction mixture was heated to 100 °C and continued stirring for two days. Initially, the pale-yellow powder was observed. After stirring overnight green solids precipitated. The green powder was filtered out. Then purified by chromatography on silica gel (EA: Methanol 100:5) to obtain a pure product as a yellow solid (0.69 g, 70%). ^{1}H NMR (400 MHz, $CDCl_3$, ppm): δ 8.65 (d, 8H, pyridyl), 7.60 (d, 8H, pyridyl), 7.50 (d, 8H, phenyl), 7.25 (d, 8H, phenyl), 7.15 (s, 4H, phenyl). ESI-MS (+): m/z 721.3 $[M+H]^+$. Elemental analysis calculated (%) for $C_{50}H_{36}N_6$: C 83.31, H 5.03, N 11.66; found: C 83.31, H 5.19, N 11.54.

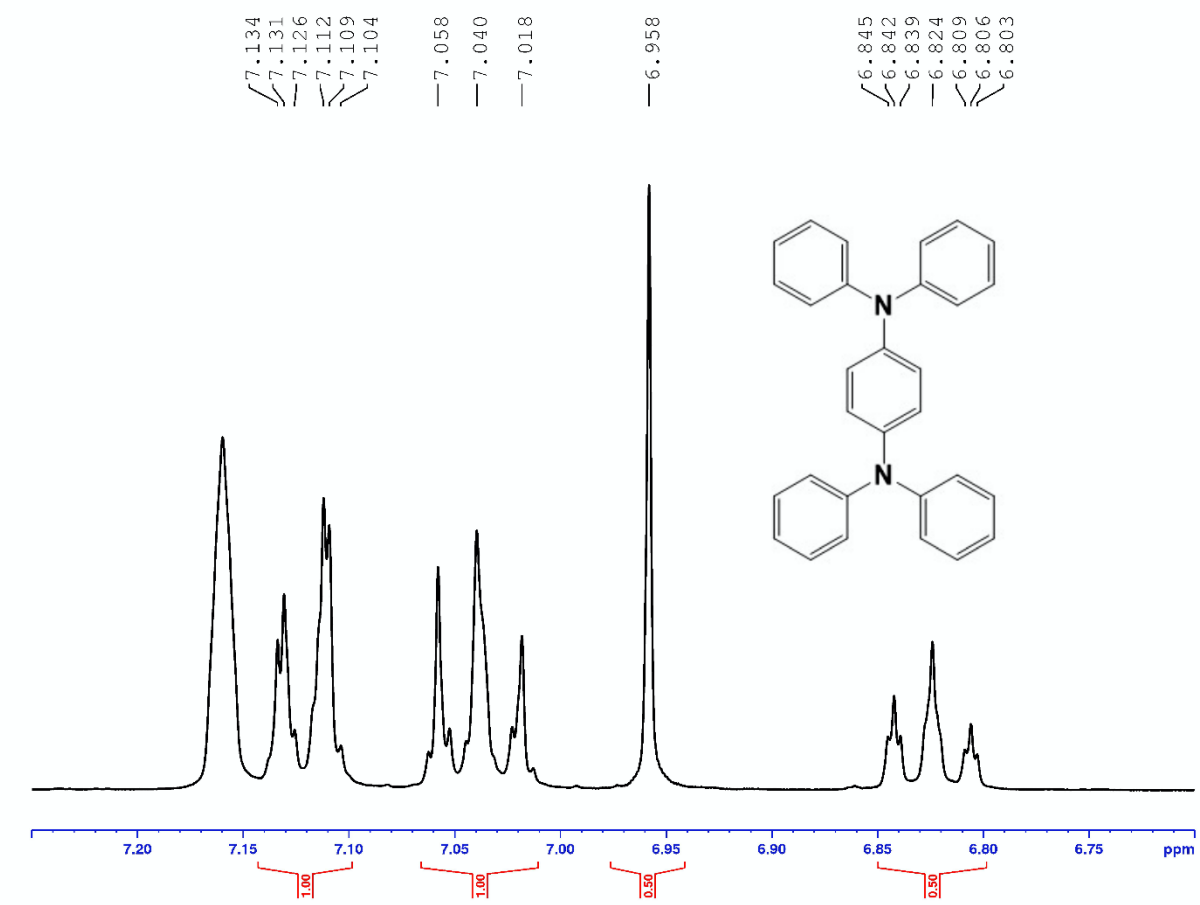

Figure S1. ^{1}H NMR (C_6D_6) of N^1, N^1, N^4, N^4-tetraphenylbenzene-1,4-diamine.

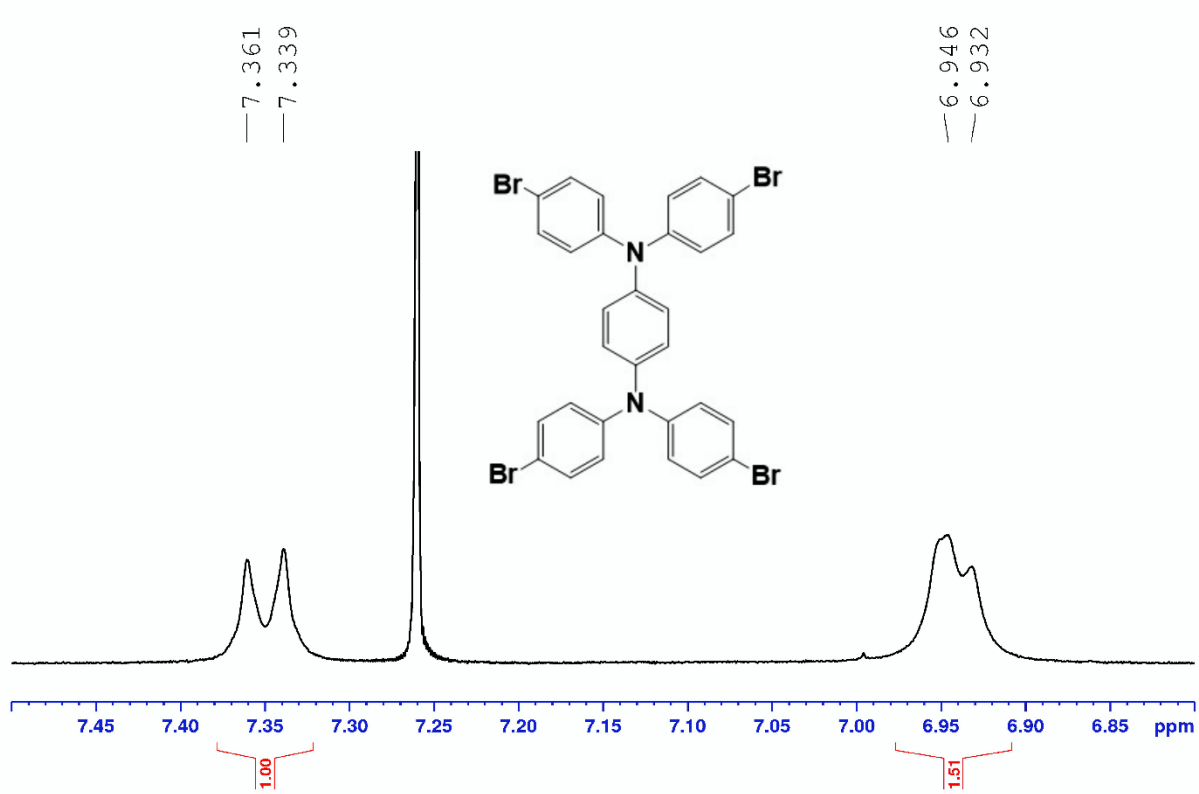

Figure S2. ^{1}H NMR ($CDCl_3$) of N^1, N^1, N^4, N^4-tetrakis(4-bromophenyl)benzene-1,4-diamine.

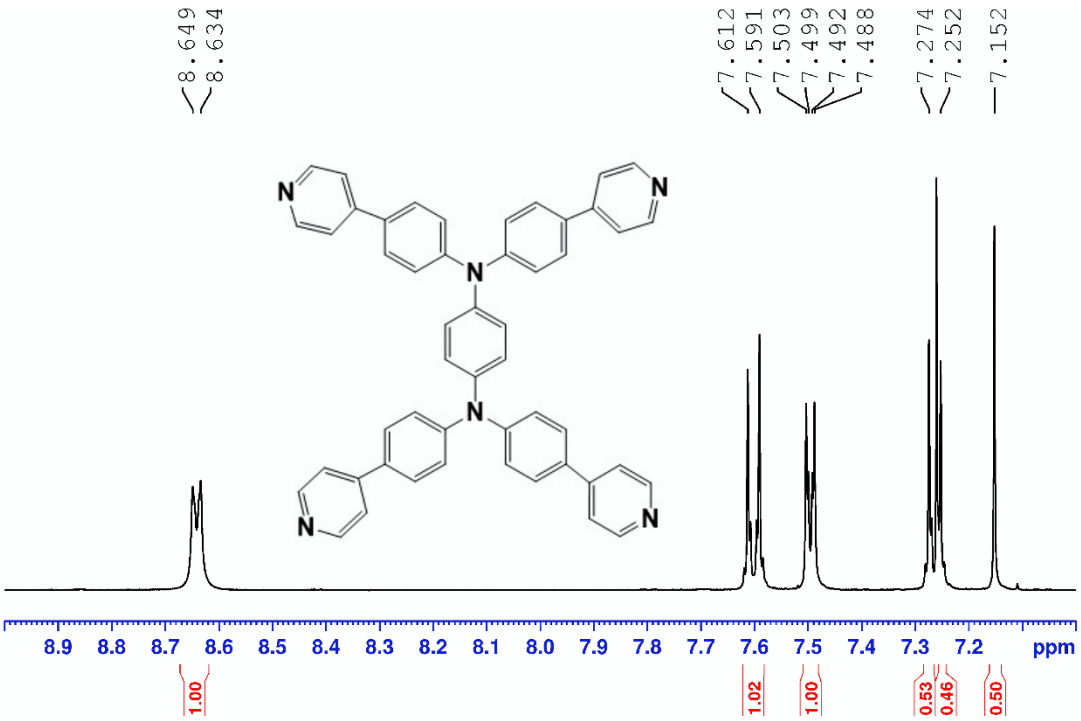

Figure S3. ^{1}H NMR ($CDCl_3$) of N^1, N^1,N^4,N^4-tetrakis(4-(pyridin-4-yl)phenyl)benzene-1,4-diamine (TPPB).

Synthesis of [Zn(TPPB)(Cl_2)]·H_2O (1)

$Zn(NO_3)_2$ (0.02 mmol, 6 mg), *N^1, N^1, N^4, N^4*-tetrakis(4-(pyridin-4-yl)phenyl)benzene-1,4-diamine (TPPB) (0.01mmol, 7.2 mg) were added to a 7 mL glass vial. DMF solvent (4 mL), conc. HCl (2 drops), water (0.5 mL), and acetonitrile (0.5 mL) were added to the glass vial, and the reaction was put at 80 °C for two days. Orange color crystals were observed. Yield (8.8 mg, 87 %). IR data (KBr, cm^{-1}) 1656sh, 1593s, 1488s, 1434w, 1323m, 1269s, 1219m, 1185m, 1070m, 1041m, 1018w, 857w, 816s, 758w, 568w, and 516w. Anal. Calcd. for $C_{25}H_{20}Cl_2N_3ZnO$: C, 58.33, H, 3.92, N, 8.16. Found: C, 57.83, H, 4.010, N, 8.34.

4) X-ray Crystallography

Crystal Structure determination

An orange prism crystal was selected and immersed in a protective oil before mounting and placed under a stream of nitrogen. Diffraction data were collected on a Bruker D8 Venture Photon III diffractometer coupled to a Smart APEX II CCD detector using a monochromated Mo K_α radiation (λ = 0.71073 Å) as a source. Absorption and other corrections were applied using SADABS. The cell constant of the Zn structure was solved using the direct method and refined using a full matrix least-squares procedure based on F^2 (SHELXL-2018). Least-squares refinement against 8852 reflections located between 5.9° and 54.08° *2θ*. Data were collected at 100(2) K. The non-H atoms in the symmetric unit were modeled with anisotropic displacement parameters. A riding atom model with group displacement parameters was used for the H atoms. Disordered solvent molecules existing in the framework were removed by SQUEEZE using PLATON[6]. CCDC 2173865

Table S1. Crystal data and structure refinement for $[Zn(TPPB)(Cl_2)]\cdot H_2O$ (**1**).

Empirical formula	C25 H18 Cl2 N3 Zn	
Formula weight	496.69	
Temperature	100.0(2) K	
Wavelength	0.71073 Å	
Crystal system	Orthorhombic	
Space group	C c c a	
Unit cell dimensions	a = 13.8231(4) Å	a= 90°.
	b = 20.1276(6) Å	b= 90°.
	c = 16.7673(4) Å	g = 90°.
Volume	4665.1(2) $Å^3$	
Z	8	
Density (calculated)	1.414 Mg/m^3	
Absorption coefficient	1.299 mm^{-1}	
F(000)	2024	
Crystal size	0.174 x 0.145 x 0.121 mm^3	
Theta range for data collection	2.161 to 27.102°.	
Index ranges	-17<=h<=17, -25<=k<=25, -20<=l<=21	
Reflections collected	56938	
Independent reflections	2584 [R(int) = 0.0850]	
Completeness to theta = 25.242°	99.8 %	
Absorption correction	Numerical	
Max. and min. transmission	0.9989 and 0.959	
Refinement method	Full-matrix least-squares on F^2	
Data / restraints / parameters	2584 / 0 / 142	
Goodness-of-fit on F^2	1.106	
Final R indices [I>2sigma(I)]	R_1 = 0.0556, wR_2 = 0.1762	
R indices (all data)	R_1 = 0.0703, wR_2 = 0.1913	
Largest diff. peak and hole	0.791 and -1.267 $e.Å^{-3}$	

$R_1 = \Sigma||F_0|-|F_c||/\Sigma|F_0|$; $wR_2 = [\Sigma w(F_0^2-F_c^2)^2/\Sigma w(F_0^2)^2]^{1/2}$

5) Physical Characterization

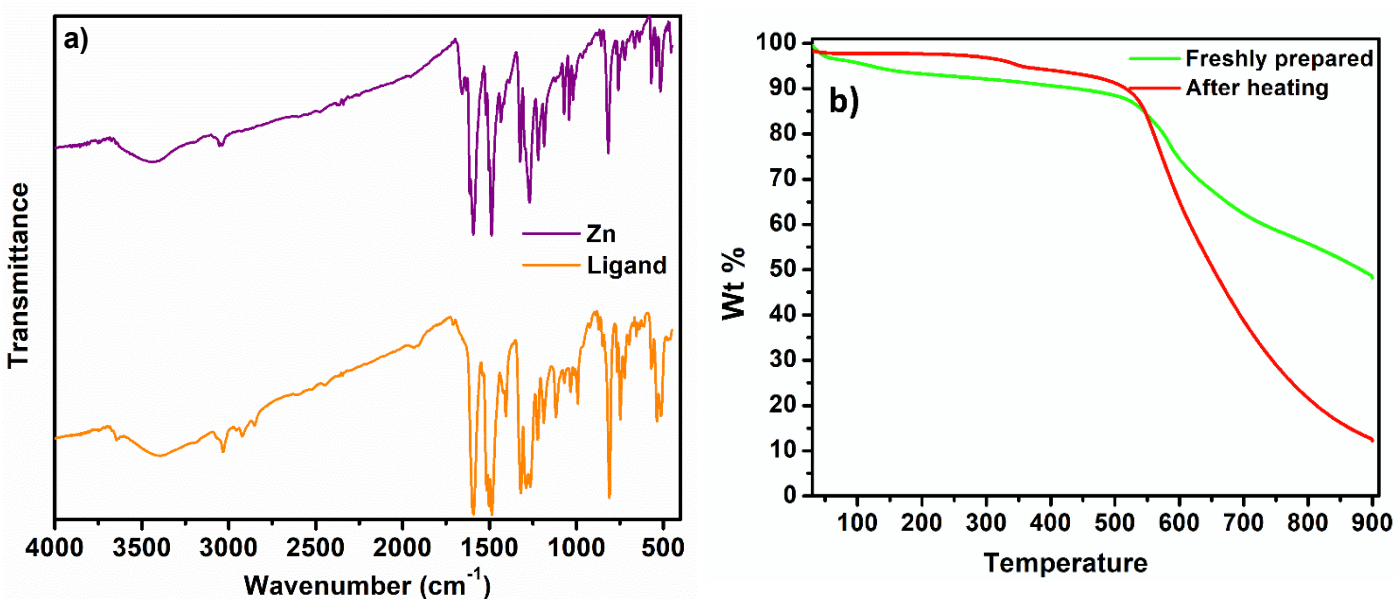

Figure S4. a) Infrared spectra for **1** and TPPB ligand, b) thermogravimetric analysis.

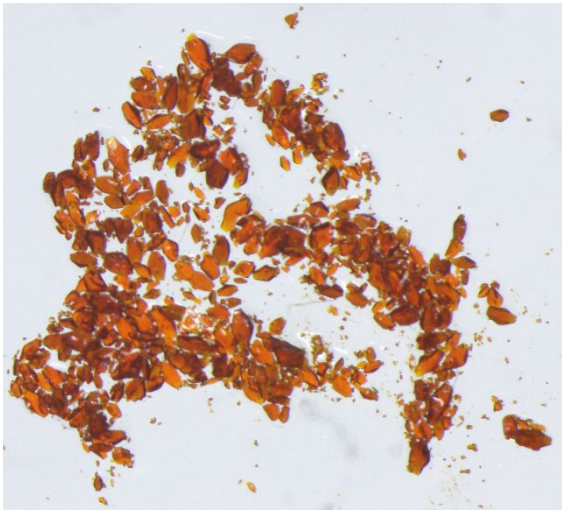

Figure S5. Crystal **1** under optical microscopy.

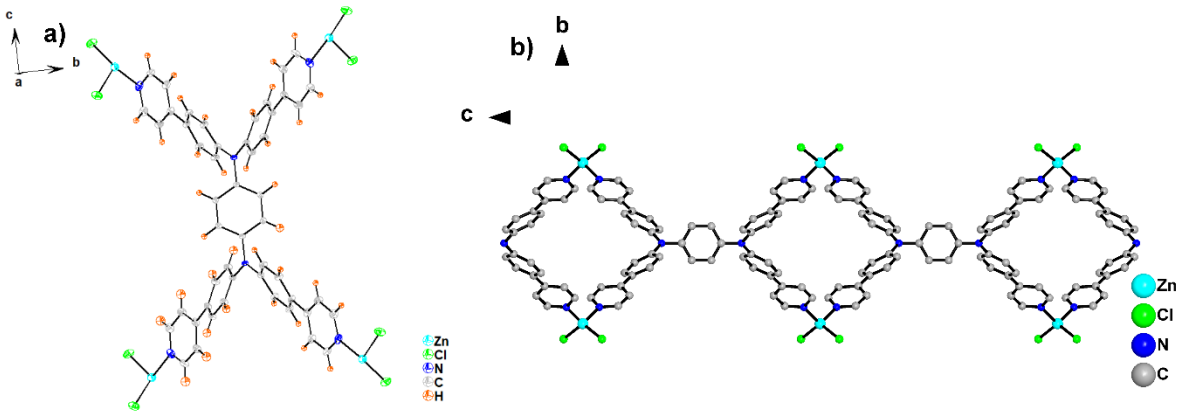

Figure S6. a) Thermal ellipsoid of **1** at 50% probability level, b) one-dimensional cage shaped along the *a* axis.

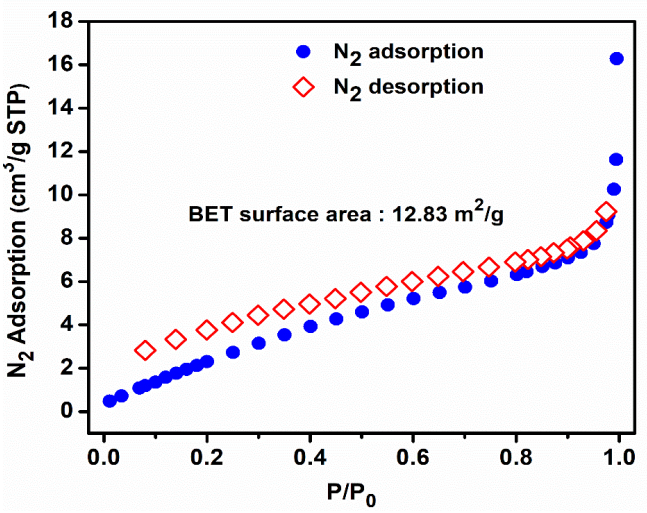

Figure S7. Nitrogen sorption isotherm of **1**. Brunauer-Emmett-Teller surface area is 12.83 m^2/g.

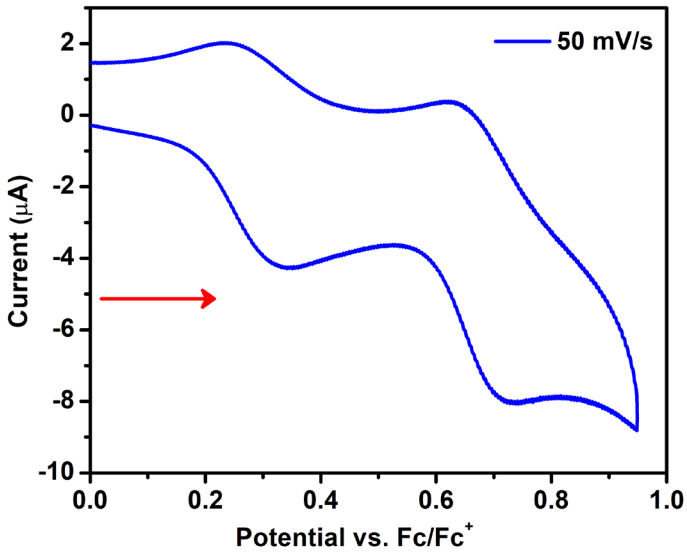

Figure S8. Cyclic voltammogram of TPPB linker in 0.1 M *n*-Bu_4NPF_6/acetonitrile.

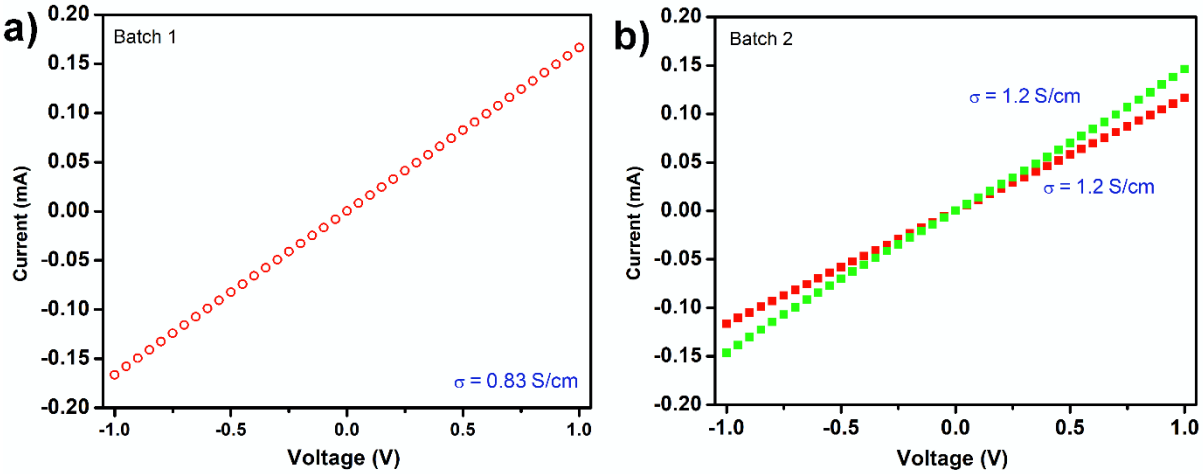

Figure S9. a) and b) IV curves measurements of **1** under different batches.

Table S2. Length, width, and thickness of **1** under different batches.

Batch	Conductivity (S/cm)	Length (μm)	Width (μm)	Thickness (μm)
1	0.83	6.6	5.4	2.4
2	1.2	2.1	1.4	1.8
2	1.2	8,8	4.6	1.8
3	1.9	3.2	0.5	1.1

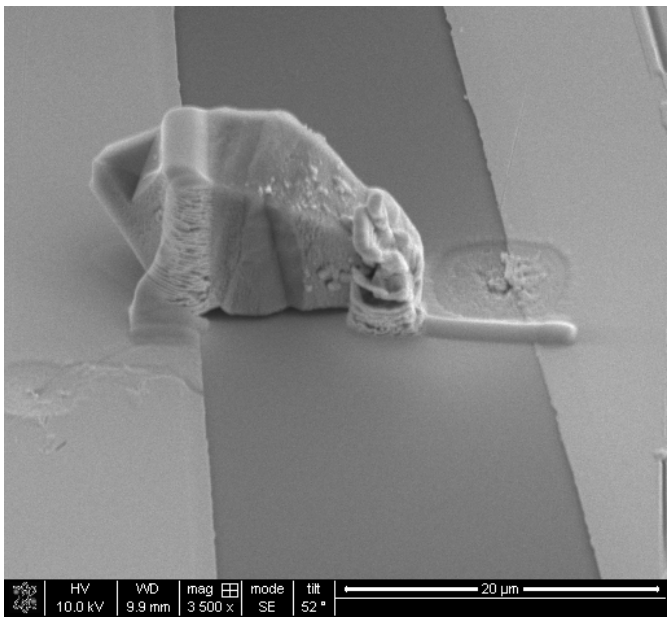

Figure S10. Scanning electron microscopy (SEM) image of **1**, platinum microelectrode fabricated using focus ion beam (FIB) at both crystal edges.

Table S3. Compilation of photoconductive gain for semiconductors.

Material	**Gain Γ, A/W**	**References**
ZnS nanobelts	0.5	*Adv. Mater.*, 2009, 21, 2034
ZnO nanospheres	5	*Small*, 2011, 7, 244
Nb_2O_5 nanobelts	6	*Adv. Funct. Mater.*, 2011, 21, 3907

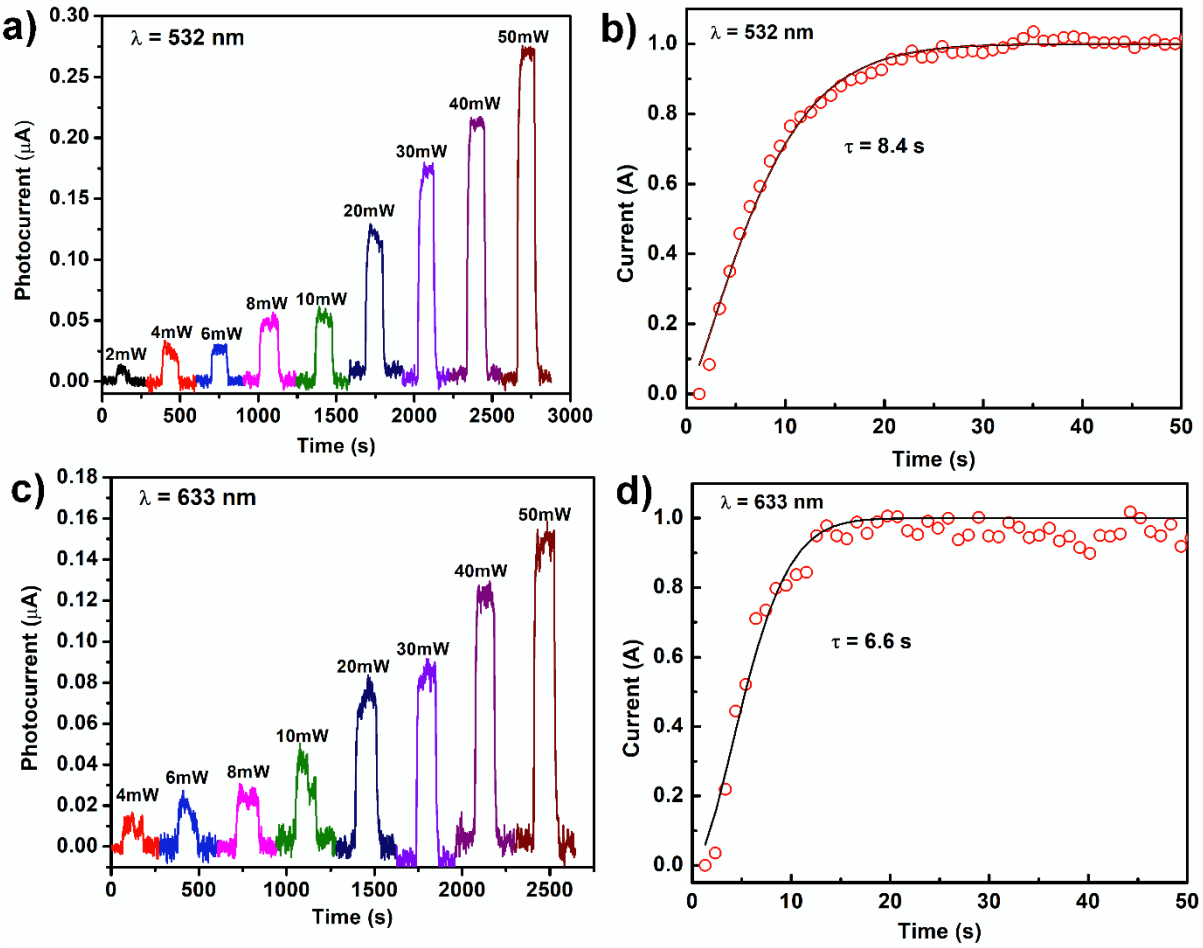

Figure S11. a) and c) Photocurrent response when time as a function at wavelength excitation of 532 nm and 633 nm, b) and d) photocarrier lifetime fitting at 532 nm and 633 nm.

6) Formula for Responsivity and Photoconductive Gain

The formula to calculate the responsivity value is $R = i_p/P$, where P is the incident optical power on the effective area of a photoconductor, i_p represents photocurrent.

For the photoconductive gain, $\Gamma = (\tau/\tau_t)$, where τ is the carrier lifetime, τ_t is the transit time between two electrodes.

[1] L. Sun, S. S. Park, D. Sheberla, M. Dincă, *J. Am. Chem. Soc.* **2016**, *138*, 14772-14782.

[2] a) G. Kresse, J. Furthmüller, *Phys. Rev. B* **1996**, *54*, 11169-11186; b) S. Grimme, *J. Comput. Chem.* **2006**, *27*, 1787-1799.

[3] a) J. Heyd, G. E. Scuseria, M. Ernzerhof, *J. Chem. Phys.* **2003**, *118*, 8207-8215; b) A. I. Inamdar, B. Sainbileg, C.-J. Lin, M. Usman, S. Kamal, K.-R. Chiou, A. Pathak, T.-T. Luo, K. S. Bayikadi, R. Sankar, J.-W. Chen, T.-W. Tseng, R.-S. Chen, M. Hayashi, M.-H. Chiang, K.-L. Lu, *ACS Appl. Mater. Interfaces* **2022**, *14*, 12423-12433.

[4] C. Wu, P. I. Djurovich, M. E. Thompson, *Adv. Funct. Mater.* **2009**, *19*, 3157-3164.

[5] D. C. Mayer, A. Manzi, R. Medishetty, B. Winkler, C. Schneider, G. Kieslich, A. Pöthig, J. Feldmann, R. A. Fischer, *J. Am. Chem. Soc.* **2019**, *141*, 11594-11602.

[6] A. Spek, *Acta Crystallograpr., Sect. C* **2015**, *71*, 9-18.